Electrical Resistivity Variations Before and After the Pingtung Earthquake in the Wushanting Mud Volcano Area in Southwestern Taiwan

Ping-Yu Chang[1], Tsang-Yao Yang[2], L. Lynn Chyi[3] and Wei-Li Hong[2]
[1]Institute of Applied Geosciences, National Taiwan Ocean University,
No. 2, Beining Rd., Keelung, 20224 Taiwan (ROC)
Email: pingyuc@mail.ntou.edu.tw
[2]Department of Geosciences, National Taiwan University,
No. 1, sec. 4, Roosevelt Rd., Taipei, 10617 Taiwan (ROC)
[3]Department of Geology, University of Akron, Akron, OH 44325-4101, U.S.A.

ABSTRACT

The extensive eruption of fluid from the mud volcanoes in the Yanchao area of southwestern Taiwan reveals the activities of the active Chishan fault. A series of time-lapse resistivity imaging measurements were initially conducted in the Wushanting Natural Landscape Preservation Area in Yanchao to evaluate the relationship between resistivity change and fault activity. Resistivity measurements were conducted first along seven 30- to 60-m survey lines to build up the regional model for mud volcanoes. We then conducted consecutive hourly and daily measurements to evaluate the short-term resistivity variations. Monthly observation was initiated along two 60-m lines in July of 2006. On December 26, 2006, two successive earthquakes with magnitudes of 6.96 and 6.99 hit the town of Hengchun in Pingtung County, about 120 km southwest of the monitoring site. Before the Pingtung earthquake, the resistivity at the research site was less than 25 ohm-m. Two regions with relatively low resistivity were found at a depth greater than 4-m at the positions of the two mud volcano craters. The two low-resistivity regions indicate the locations of conduits for the mud fluid. The major changes of resistivity are located in the vadose zone between the surface and a depth of 3-m. After the Pingtung earthquake, the maximum resistivity increased in the vadose zone by 7 ohm-m and 20 ohm-m on survey lines D and E, respectively. In the zone, the estimated water content of D and E decreased by 7% and 10%, respectively, after the earthquake. We suggest that the decrease of resistivity in the vadose zone most likely reflects the decrease of water content, itself caused by the earthquake tremors' increased emission of gas. Currently, we are continuing the resistivity-monitoring surveys and hope to provide more data to clarify the seasonal-variation patterns and to compare them with the previous findings.

Introduction

Mud volcanoes are geological features distributed in a wide variety of tectonic environments, such as passive continental margins, continental interiors, and transform and convergent plate boundaries (*e.g.,* Hedberg, 1980; Fertl and Timko, 1970; Higgins and Saunders, 1974; Reed *et al.,* 1990). In southwestern Taiwan, abundant mud volcanoes have erupted on land and offshore owing to the intense compression tectonic environment (Shih, 1967; Huang *et al.,* 1992; Liu *et al.,* 1997). Most mud volcanoes on land are related to geological structures and are distributed along the axis of the Gutingkeng anticline and the Chishan fault (Wang, 1988). The gas in mud volcanoes is believed to be closely related to decomposed organic matters in the mudstone formation. You *et al.* (2004) suggest that fluid emanating from Taiwanese mud volcanoes were originally marine pore waters that mixed with meteoric water, or that underwent surface evaporation during the recharge and discharge processes. Nevertheless, the gas-eruption activity of mud volcanoes are found to be closely related to tectonic activity (Sung *et al.,* 2004). It is difficult to estimate the gas volume correctly given the government restrictions on setting up any permanent instruments in the field, therefore it is necessary to look for other ways to monitor the gas-eruption activities quantitatively. In theory, the volume occupied by gas is more resistive than the water-saturated soil volume. If the eruption activity increases, the occupied gas volume should also increase. This premise makes it reasonable to measure the gas-eruption activity through electrical resistivity differences.

Electrical resistivity surveys employ a direct current or an alternating current of very low frequency and measure the variation of spatial potential fields to explore the distribution of the ground's apparent resistivity. Techniques for electrical resistivity monitoring have been successfully used for environmental purposes because of the techniques' abilities to identify resistivity changes stemming from either water-content variation in the vadose zone or the migration of contaminants (*e.g.,* Kean *et al.,* 1987; Van *et al.,* 1991). In this study, we attempt to quantify the mud volcano activity in the Wushanting Natural Landscape Preservation Area with surface electrical resistivity imaging profiling technology. The study was divided into three phases. In the first phase, we deployed seven survey lines, including four south-to-north 60-m long and three east-to-west 30-m long resistivity survey lines to investigate the background near-surface geology in the WNLPA. In the second phase, we collected hourly and daily time-lapse resistivity measurements along two survey lines to analyze the range of short-term variation. The design of the second phase is to study how the resistivity varies in a short period. The third phase included monthly measurements over a 10-month period to identify the long-term variation of the mud volcano activities, and to compare the resistivity variation with the tectonic activity.

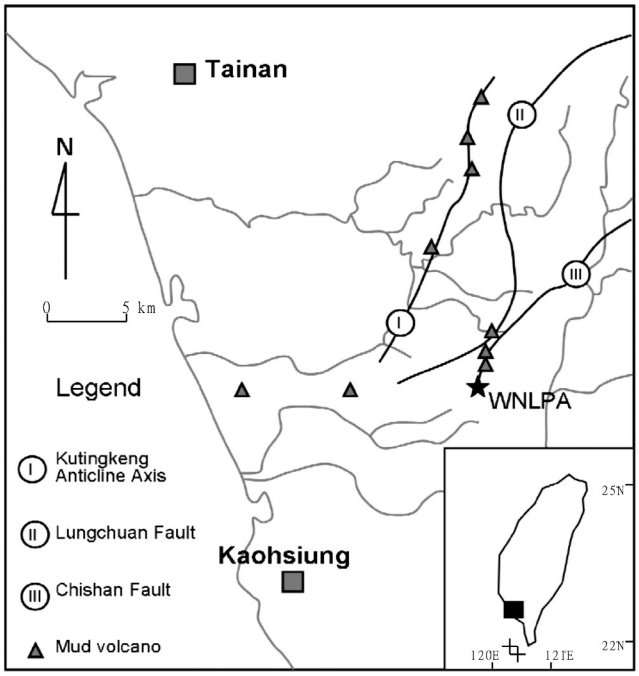

Figure 1. Regional maps showing the locations of mud-volcano groups (LC, TKS, AKS, KSP, LYS, and WST) in southwestern Taiwan. The star sign shows the location of the Wushanting Natural Landscape Preservation Area (WNLPA) site. The Cross labels in the lower right small map indicate the two epicenters of the Pingtung doublet earthquake.

Site Description

Taiwan is located at the boundary of the Philippine Sea plate and the Eurasia plate. At least 17 major mud volcano sites can be identified in southwestern Taiwan. Among them, the Wushanting Natural Landscape Preservation Area (WNLPA) (Fig. 1) is located near the Chishan fault in Yanchao, Taiwan. The eruption of fluids and gases from the fissures in the thick Gutingkeng mudstone resulted in two huge cone-shape landscape features. The Gutingkeng formation is mainly Pleistocene marine gray mudstone intercalated with thin-bedded sandstone (Keng, 1981), and clay particles can constitute about 59% of the formation's content. The thickness of the formation reaches is over 5,000 m.

The mud volcanoes in the WNLPA are located in a 200-m $\times$ 150-m platform (Fig. 2(a)). There were originally three main mud volcano craters in the platform. A new eruption crater was formed beside the B crater after the Pingtung earthquake in December 2006. Constantly erupted mud fluids almost entirely eliminate plants from the ground near the craters. The unique geomorphic features have led the government to designate the WNLPA site a natural landscape preservation area in the county.

We chose the surface electrical resistivity imaging profiling (RIP) method for this study because government policies prohibit establishment of permanent instrumentation in the WNLPA. The LGM 4-point Light hp resistivity meter and ActEle system (Lippmann, 2005) were used for the field resistivity measurements. For the resistivity measurements in the first phase, we selected dipole-dipole and Wenner arrays because they provide lateral and vertical coverage of the subsurface. To construct the geology model of the WNLPA site, we performed data acquisition with 40 electrodes spaced at 1.5-m intervals along the south-to-north lines (lines C, D, E, and F in Fig. 2(b)), and with 20 electrodes along the east-to-west lines (lines X, Y, and Z in Fig. 2(b)). To address the lateral resistivity variation and to use our survey time efficiently, we used only the dipole-dipole method during the second and the third phases of the research. In the second phase, we conducted measurements along the D and E lines with the same 1.5-m electrode spacing to monitor short-term variations in resistivity. The short-term monitoring was conducted in two different time frames: first we carried out monitoring every hour for 8 consecutive hours, and then we resumed the monitoring, carrying it out once a

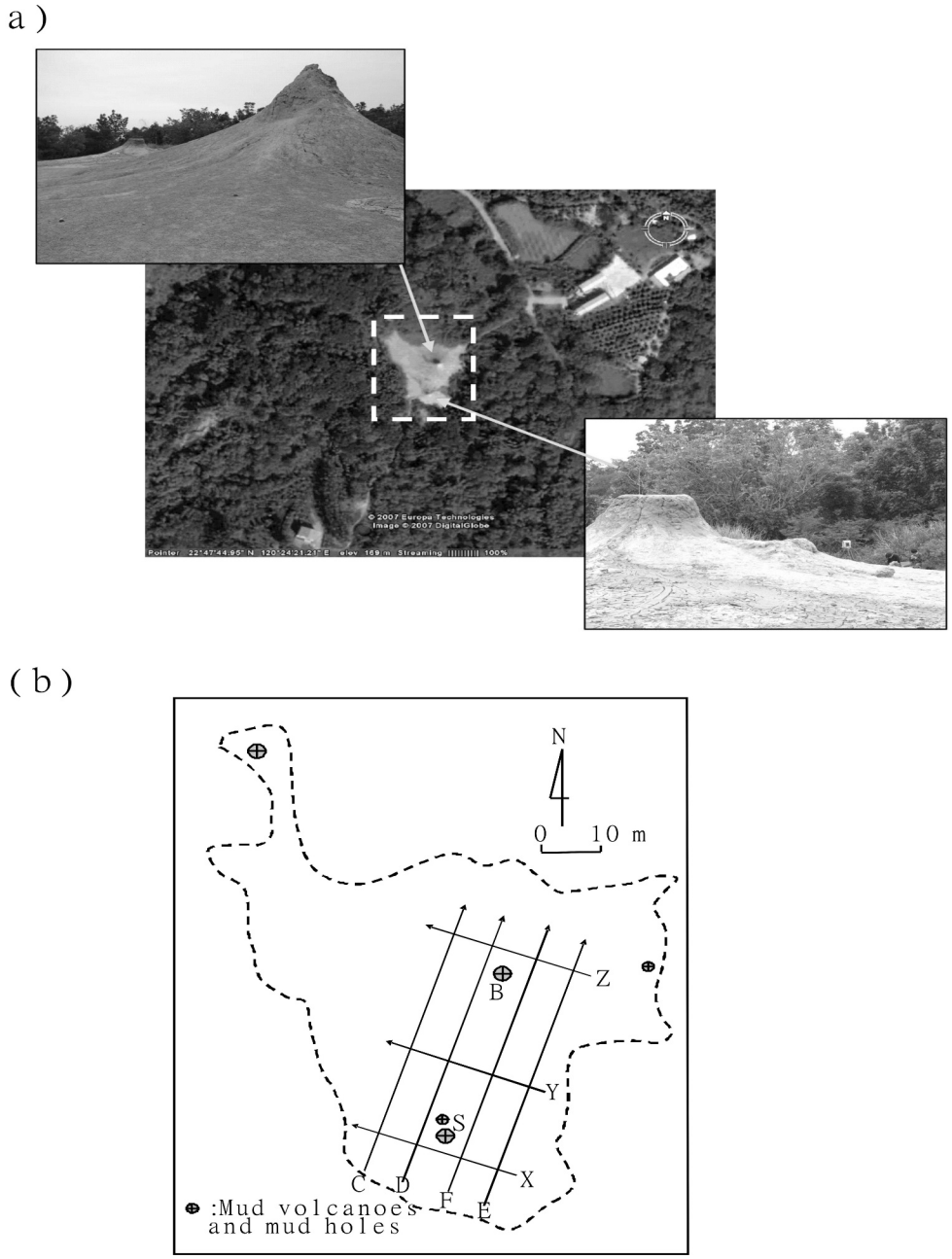

Figure 2. (a) Satellite image of the WNLPA (from Google^{TM} earth) and pictures of the mud volcano B (upper left) and mud volcano S (lower right). (b) Resistivity survey plan of the WNLPA site (dotted line indicates the range of the WNLPA). B and S mark the locations of two major mud-volcano craters. Resistivity surveys were conducted along the C, D, E, and F lines and along the X, Y, and Z lines. Arrows show the survey direction.

day for one week. In the third phase, we collected resistivity data along the D and E lines with the same 1.5-m electrode spacing for 10 mo. Because precipitation may affect the resistivity measurements, we took no resistivity measurements during the three days following significant rainfall; in this way, we sought to avoid a situation where the precipitation would affect our long-term monitoring study. As a result, the frequency of the long-term measurement was roughly once a month, with the frequency varying in relation to weather conditions. Resistivity data were inverted with EarthImager^{TM} 2D software (AGI, 2006), which uses a forward modeling subroutine and non-linear optimization techniques to calculate resistivity values.

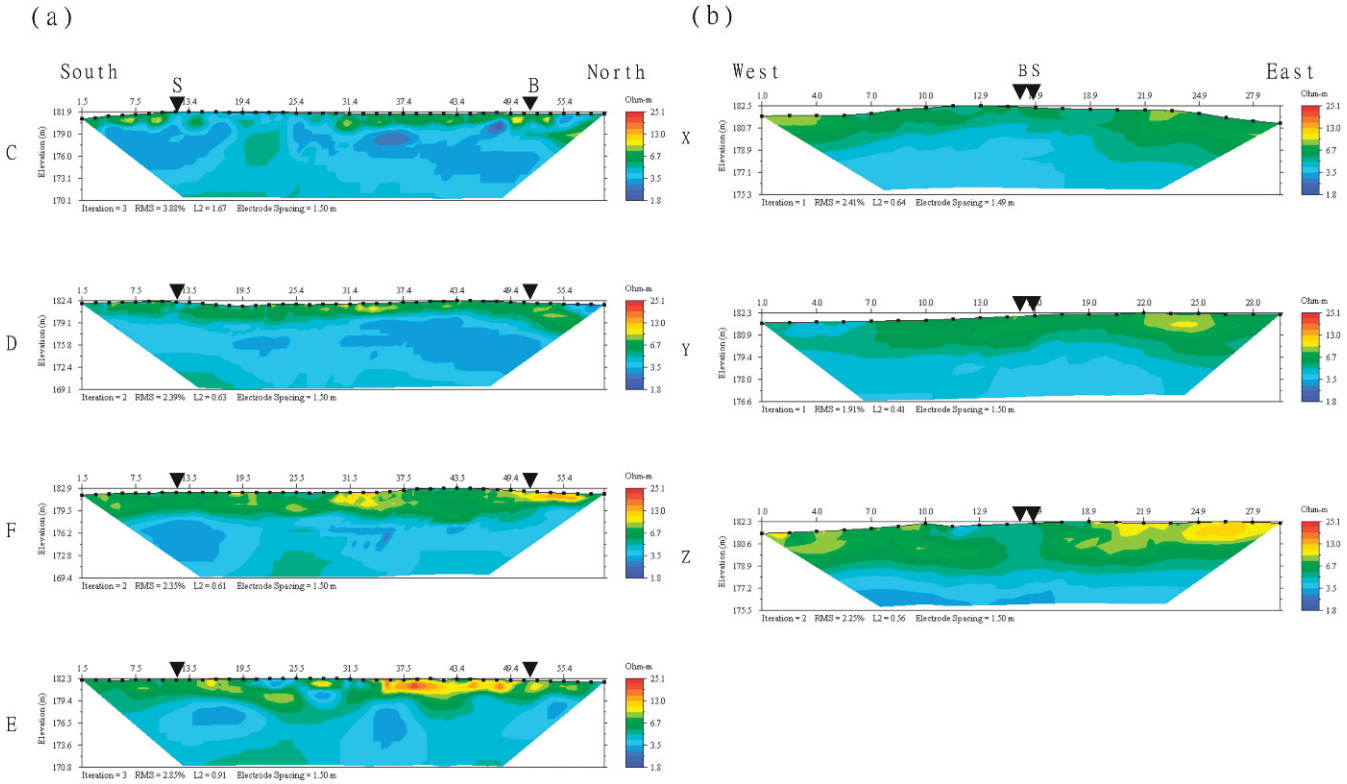

Figure 3. (a) Inverted resistivity imaging profiles of the north-south C, D, E, and F lines collected at the WNLPA site in July 2006. B and S indicate the projected locations of the two mud-volcano craters. (b) Inverted resistivity images of the east-west X, Y, and Z profiles.

Results

Background Resistivity

The dipole-dipole and Wenner-resistivity surveys were conducted on July 22, 2006 (during the first phase), to construct the background model of the WNLPA site. The acquired dipole-dipole and Wenner data were then combined and inverted together using the AGI EarthImager^{TM} 2D software (AGI, 2006). Figure 4 shows the inverted resistivity of the north-south C, D, E, and F lines and the east-west X, Y, and Z lines. Symbols B and S indicate the projected positions of the mud volcano craters. The horizontal distance, shown in images in Fig. 3, indicates the displacement from the position of the reference electrode in each survey line. Because lines C, D, E, and F (Fig. 3(a)) had longer survey distances, and therefore allowed for larger electrode spacing, the resistivity-exploration depth for lines C, D, E, and F is larger than that for lines X, Y, and Z (Fig. 3(b)). In general, the inverted resistivity ranged from 2 to 16 ohm-m for the mudstone in the WNLPA site. The vadose zone, which is located at the surface and is more resistive than the underlying saturated layer, is about 2–3 m thick in the study area. Regarding high resistivity regions (regions wiyh resistivity greater than 10 ohm-m), lines E and F exhibited resistivity values greater than the resistivity in the C and D lines. Line Z exhibited resistivity that was greater than the resistivity in lines X and Y. Because of the geology in the WNLPA site, these regions may constitute a ‘‘drier zone’’ than the rest of the vadose zone. We located low resistivity regions (regions with resistivity less than 4 ohm-m) under the two mud volcano craters in lines D, E, and F. Because the mud volcanoes are still emitting gas and mud fluids from craters, the low resistivity region may indicate the presence of fissures where the mud fluids existed.

Results from surveys along lines C, D, E, and F were combined together, and the data between lines were then interpolated with the simple kriging method; in this way, we formed the resistivity layered model of the WNLPA site shown in Fig. 4. In Fig. 4, a high resistivity region (with resistivity over 10 ohm-m) appears in the southeast part of the WNLPA within 4-m of the surface. Compared to the rest of the area, the drier region is located in the high ground formed by the mud emitted from the mud volcanoes. This region’s characteristics imply that the southeast WNLPA site has a thicker vadose zone with less water content above the shallow water table. Regarding the mudstone deeper than 4-m, we identified two isolated low-resistivity

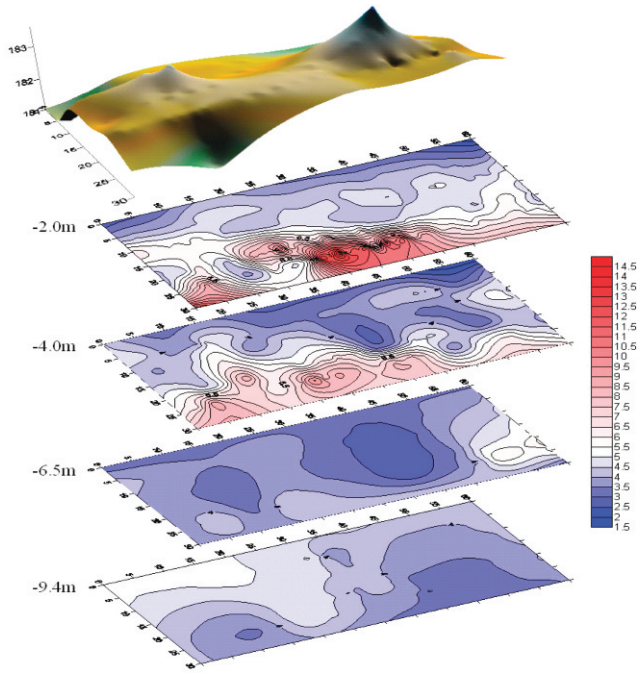

Figure 4. Background resistivity images collected at the WNLPA site in July 2006. The resistivity image of each different depth was created by applying the kriging method to the inversion results from the C, D, E, and F lines and from the X, Y, and Z profiles.

regions (with resistivity less than 4 ohm-m) under the two mud volcano craters. The location-related consistency between the very low resistivity region in the deeper subsurface and the mud volcano craters on the ground surface suggests fissure conduits of oversaturated mud are present.

Short-term Variation of the Resistivity

The short-term (daily) resistivity variations were monitored prior to monitoring the long-term (monthly) resistivity changes. Evaluation of the short-term variations allowed us to distinguish the accumulated long-term deviations from the hourly or daily variations. Dipole-dipole surveys were first conducted along line D every hour for 7 consecutive hours to assess the variation from hour to hour. Figs. 5(a)–(b) show the average resistivity and the standard deviation of the hourly surveys, respectively. Figure 6(a) shows that the resistive layer exhibiting resistivity over 5 ohm-m has a depth less than 3 m. Furthermore, regions with higher resistivity (>9 ohm-m) are located at the positions near the two mud volcano craters. Also, as Fig. 5(b) shows, most of the line D's standard deviation values in the 7-hour period are less than 1 ohm-m. The maximum standard deviation is about 4.0 ohm-m and is found only at two surface points, located at 13-m and 44-m from the reference electrode. The hourly observation shows no significant resistivity variation during the study period. This

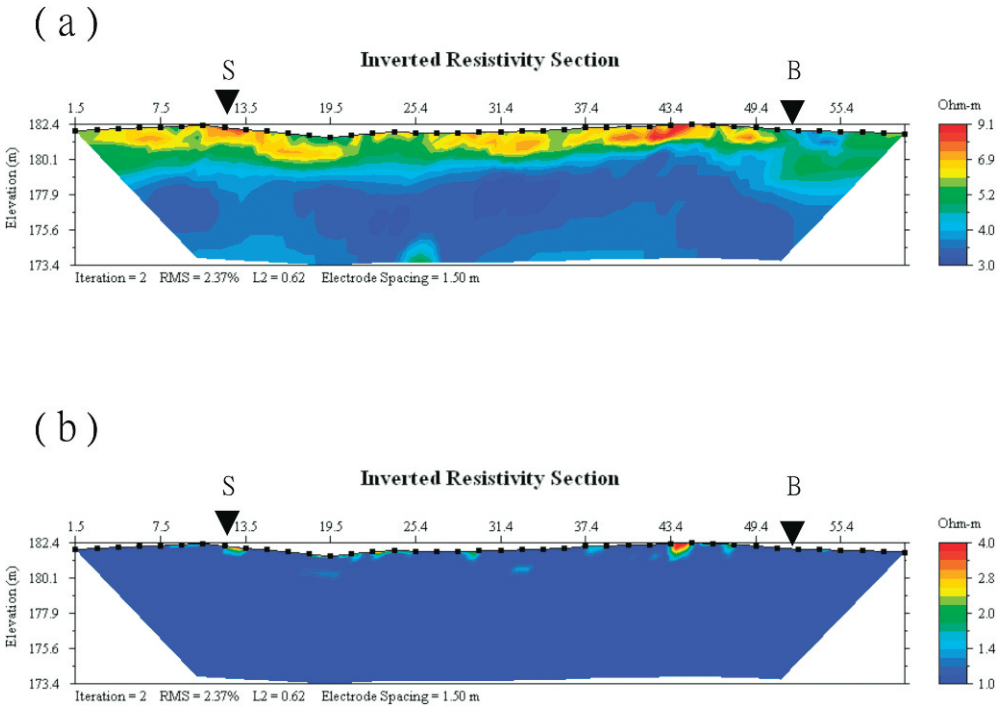

Figure 5. (a) Average resistivity of the hourly surveys along the D line. (b) Standard deviation of resistivity of the hourly surveys along the D line.

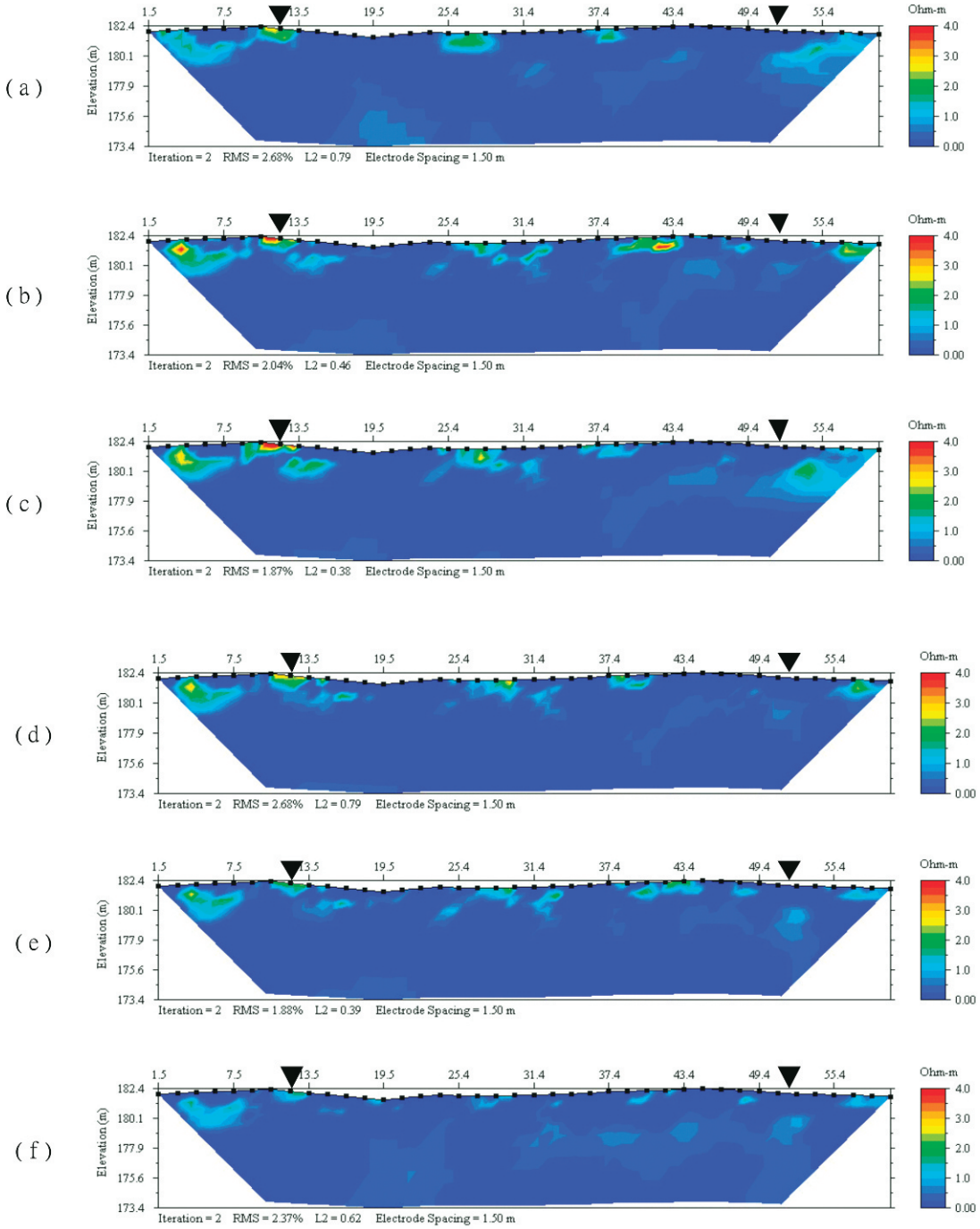

Figure 6. Resistivity difference in the background data collected at (a) day 2, (b) day 3, (c) day 4, (d) day 5, (e) day 6, and (f) day 7 in the 7-day observation study.

finding implies that the influences from the hourly change of climate conditions are minor during the observation period along the D profile.

After the completion of hourly observations on day 1, we commenced the daily observation for six consecutive days. During the entire 7-day period, there was no precipitation in the study area. Figures 6(a) to 6(f) illustrate the resistivity difference with respect to the background at day 1. Figure 6(a) illustrates the finding that, at day 2, regions exhibiting sporadic resistivity-related changes over 1 ohm-m appeared near the surface locations. The precise ranges of these locations are as follow: from 1.5-m to 4-m, from 10-m to 13.4-m, from 25.4-m to 27.4-m, from 37-m to 38-m, and from 55.4-m

to 59.5-m. Most of the regions were not deeper than 3-m from the surface (Fig. 6). At day 3, the region between 37-m and 38-m broke down into several smaller regions, and the rest of the regions' maximum changes in resistivity increased to over 2.5 ohm-m (Fig. 6(b)). Regarding the region that was from 10-m to 13.4-m, the maximum change in resistivity increased to over 4 ohm-m at day 4 (Fig. 6(c)) and then decreased to about 3.0 ohm-m by day 5 (Fig. 6(d)). Figures 6(e) and 6(f) illustrate the same trend of decreasing resistivity as that at day 5 for all anomalous regions at day 6 and day 7.

Our examination of daily variations has helped us to evaluate the range of daily variation and the trend of daily resistivity change. In summary, the results of our daily resistivity observations indicate that most of the anomalous resistivity regions during the 7-day period were located no deeper than 3-m from the surface. The daily resistivity change varied systematically between 2 ohm-m and 5 ohm-m at the WNLPA site. The absence of drastic daily resistivity variation over 5 ohm-m implies that the resistivity variation at the WNLPA site is progressive and that the long-term resistivity change over this range can be viewed as the consequences of accumulated short-term changes, rather than as short-term peaks.

Monthly Variations in Resistivity

It was expected that the resistivity change of mud volcanoes would take place around the vertical fault fissures, as mentioned in the previous section. Therefore, we used RIP measurements with the dipole-dipole electrode configuration along the D and the E survey lines. The observation period extended from July 2006 to April 2007. During the long-term observation, two successive earthquakes with magnitudes of 6.96 and 6.99 hit southern Taiwan offshore of the Hengchun twon, Pingtung County, on December 26, 2006 (Chen *et al.,* 2008). The epicenters of the Pingtung doublet earthquake were about 120 km southwest of the WNLPA site (locations of epicenters of the Pingtung doublet earthquake are indicated in Fig. 1). In the WNLPA area, earthquake magnitude measured is about 5 (CWB, 2006) for the Pingtung earthquake. This major earthquake constituted an extraordinarily useful event for our long-term resistivity study. Therefore, we took two additional measurements immediately after the earthquake to evaluate whether or not the earthquake significantly affected the activity of the mud volcanoes.

Based on background that we collected on July 22, 2006, Fig. 7 illustrates (1) the inverted long-term resistivity of the D profile and (2) the difference between the observed resistivity and the background. The resistivity images of the D profile show that a relatively resistive zone (resistivity higher than 5 ohm-m) existed at the shallow subsurface above 181 m (about 0-m to 3-m in depth). We had identified this resistive region as the near-surface vadose zone in the study's first phase. Before the Pingtung earthquake (Dec. 26 2006), the major resistivity increase was in the vadose zone. Several regions with resistivity anomalies less than 5 ohm-m appeared sporadically in the vadose zone. In general, the resistivity change before the earthquake was less than the range of the short-term variation. Two days after the Pingtung earthquake, the maximum resistivity increase reached about 10 ohm-m, twice the short-term variation range in the D profile. A similar increased resistivity in the shallow subsurface was reported by Yang *et al.* (2002) after the Chi-Chi earthquake in the hanging wall of the Chelungpu fault zone. By April 14, 2007, the measured resistivity anomaly increased to over 12 ohm-m near the S mud volcano crater. Unfortunately, we did not have the day-to-day measurements to verify whether these data reflected the real resistivity change near the S mud volcano crater or were simply data offset owing to an unidentified equipment-setup problem.

Figure 8 shows the resistivity images and the resistivity difference to the background of the E profile. The images show that several anomalous resistivity regions were developing above 3-m in depth in the vadose zone throughout the monitoring period. The maximum resistivity anomaly gradually increased and reached about 12 ohm-m by December 17, 2006. On December 28, two days after the Pingtung earthquake, the E profile's maximum resistivity increased to over 20 ohm-m near the surface. The earthquake-induced increase in the E profile's maximum resistivity was about three times larger than that of the nearby D profile's maximum resistivity. The maximum resistivity increases were over 20 ohm-m on January 14 and February 28 in 2007, but only slightly greater than 15 ohm-m on April 14, 2007. In conclusion, the E profile's resistivity in the vadose zone increased to over 20 ohm-m owing to the Pingtung earthquake, and slightly decreased four months after the earthquake.

Discussion

There are many possible reasons for the changes in resistivity; such as temperature, precipitation, earthquake activity, and their subsequent influence (namely, gas or fluid emissions from the subsurface). Since we did not take measurements within three days following precipitation events, we should be able to rule out precipitation influence. Besides the precipitation, the temperature may affect the resistivity variations. After examining the daily temperature records during the monitoring period (Fig. 9), we concluded that the resistivity roughly decreases by about 0.7 ohm-m when

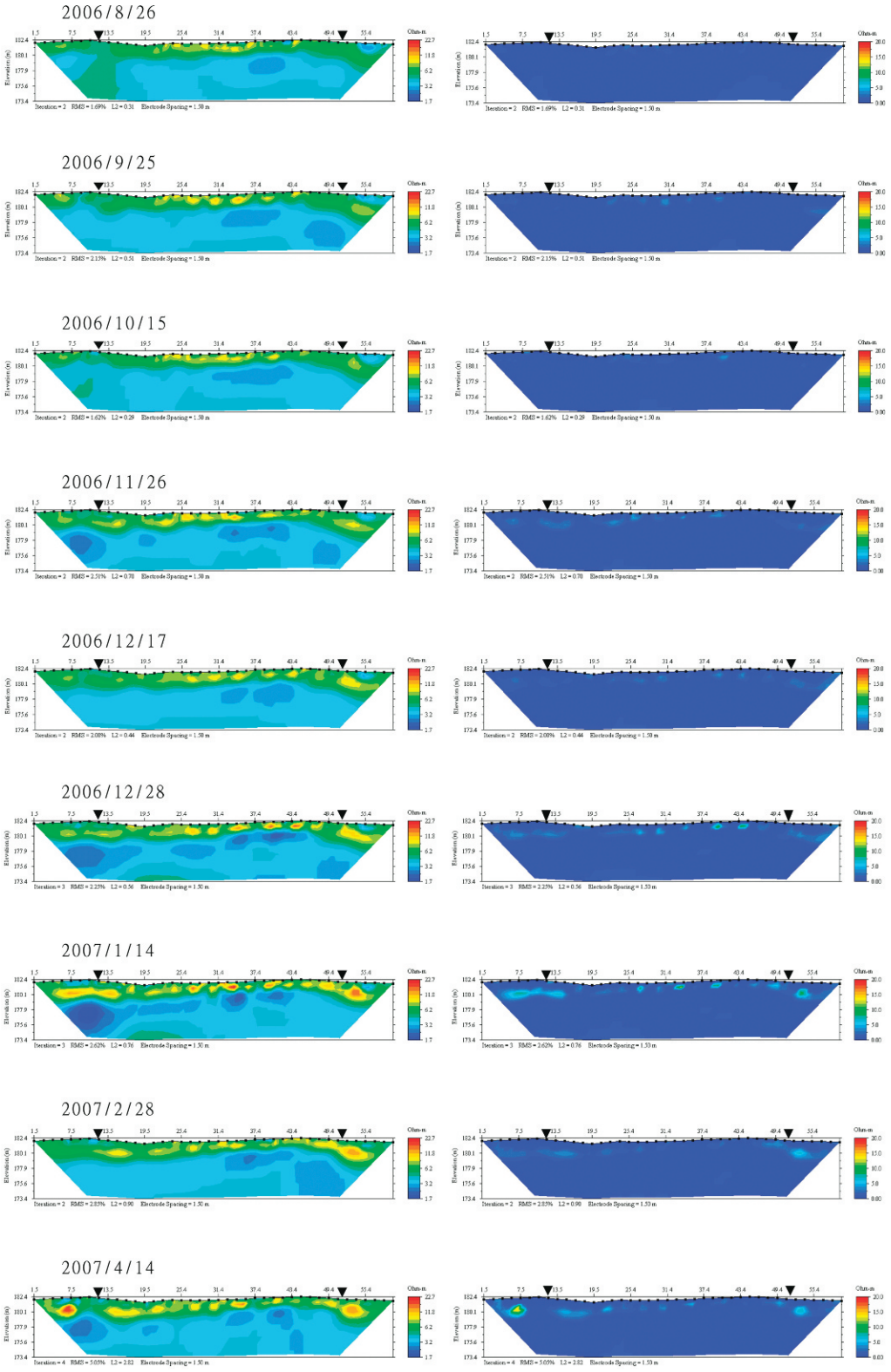

Figure 7. Left: the inverted resistivity images of the D line with respect to the long-term monthly observation. Right: the resistivity difference of the D line to the background data (July 22, 2006).

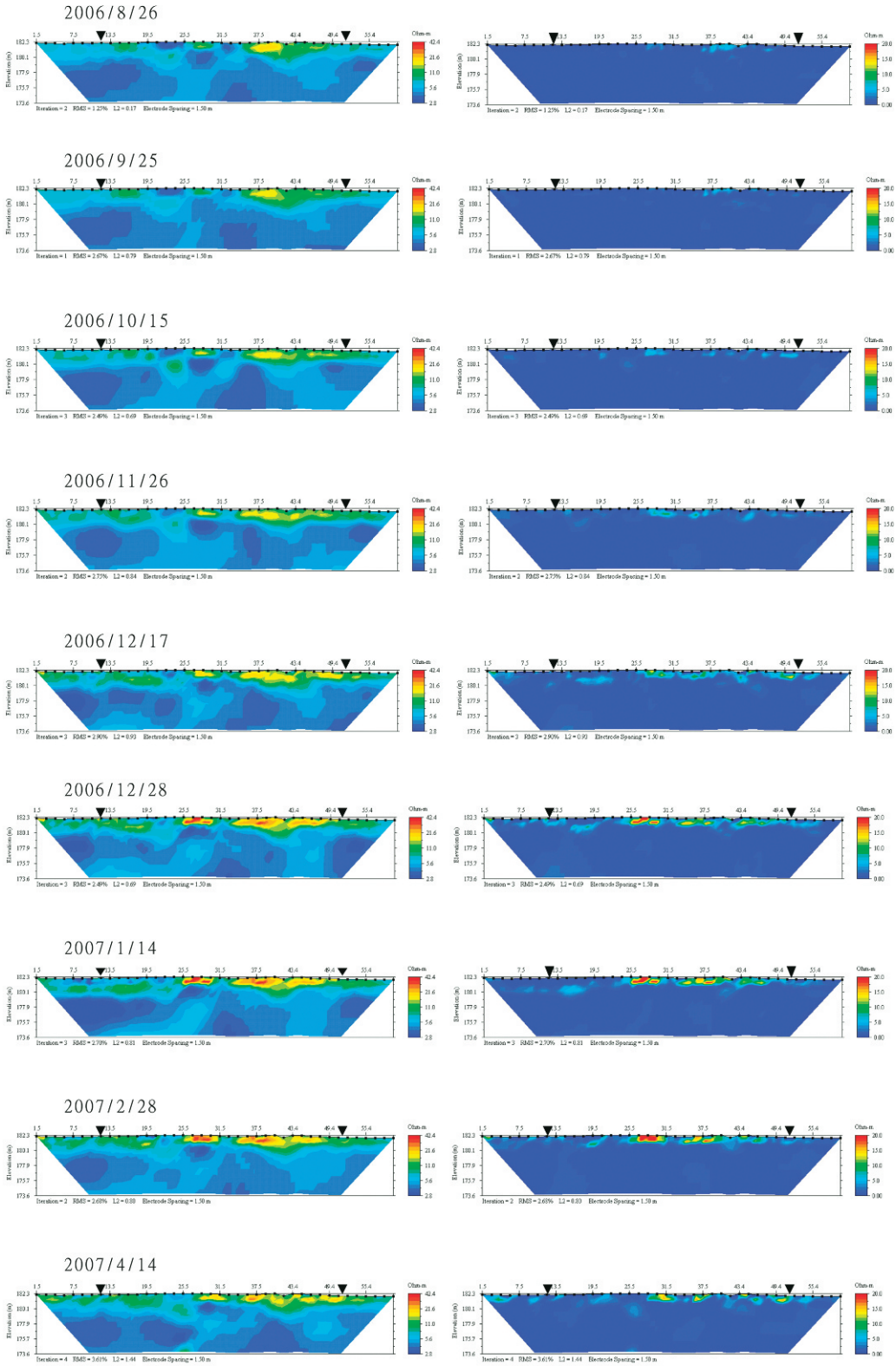

Figure 8. Left: the inverted resistivity images of the E line for long-term monthly observations. Right: the resistivity difference of the E line with respect to the background data (July 22, 2006).

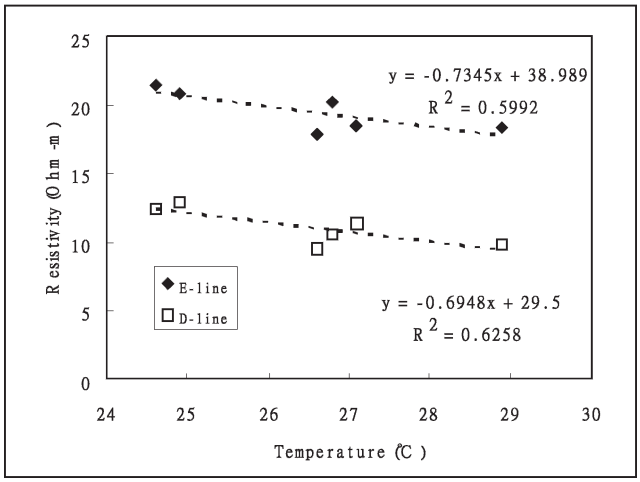

Figure 9. Comparison of maximum resistivity of D and E lines and the ground temperature before the Pingtung earthquake. Dashed lines are the regression lines of the D and E profiles.

the daily average temperature increases by 1°C. The temperature was not likely the major factor causing the abrupt resistivity decrease after the Pingtung earthquake since the average temperature only decreased 5–7°C in December at the WNLPA site. Therefore, we suggest that the decrease of resistivity in the vadose zone of the D profile and the E profile most likely stemmed from the earthquake activities.

In addition, there is a radon activity monitoring site located about 500 m south of the WNLPA in the Campus of National Kaohsiung Normal University. Figure 10(a) shows the variations of radon activities during 2006 and 2007. Unfortunately, the instrument appears to encounter some problems in recording the radon data in July and August of 2006 and also in February of 2007. We found that the radon activity recorded by the instrument seems to have gradually recovered to a steady state after October 2006. In Fig. 10(b), we show the half-week maximum radon activity from October 2006 to January 2007. The peak values of the radon activity variations seem to be correlated well with the highest and lowest temperatures of every month, except for the peak appearing at the time of the Pingtung earthquake. Although the radon activities are affected primarily by the temperature, the extraordinary peak at the Pingtung earthquake suggests excess gas emission in the area. We further compared the resistivity at 1.2-m deep to the methane gas flux collected by Hong *et al.* (2009) at the surface in WNLPA. Methane

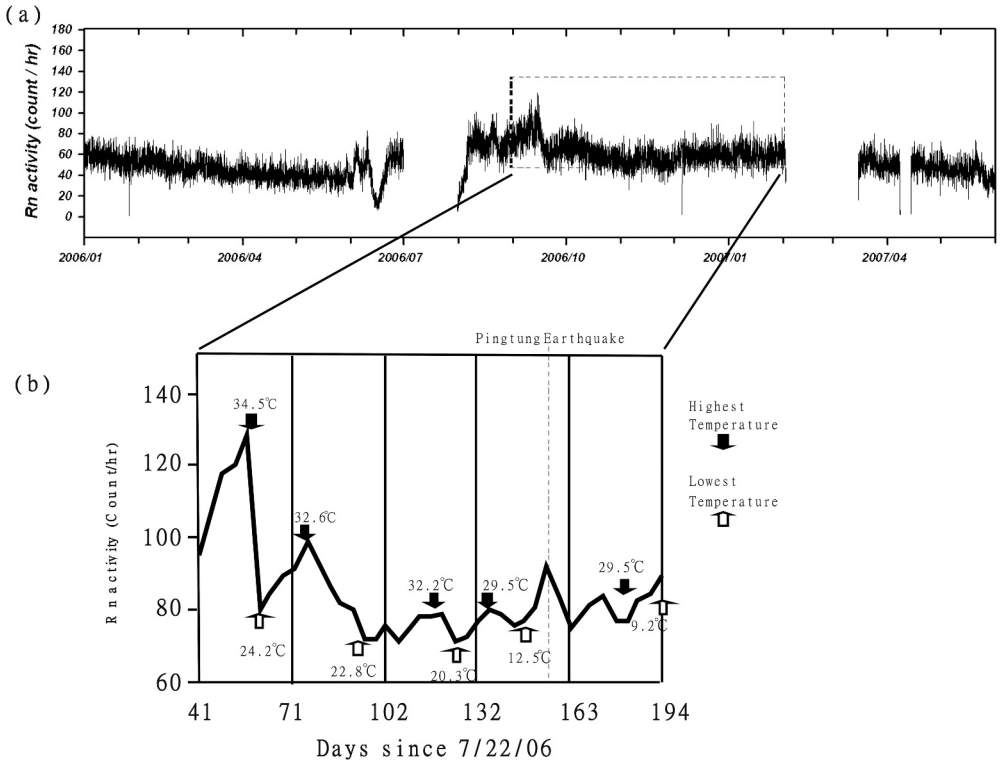

Figure 10. (a) Radon activity records during 2006 and 2007. (b) Variation of half-week maximum radon activities from October 2006 to January 2007. Black arrows show the highest temperatures of the month, and white arrows show the lowest temperature of the month. (The time scale is converted into days since 7/22/06 to be compared with the resistivity variations).

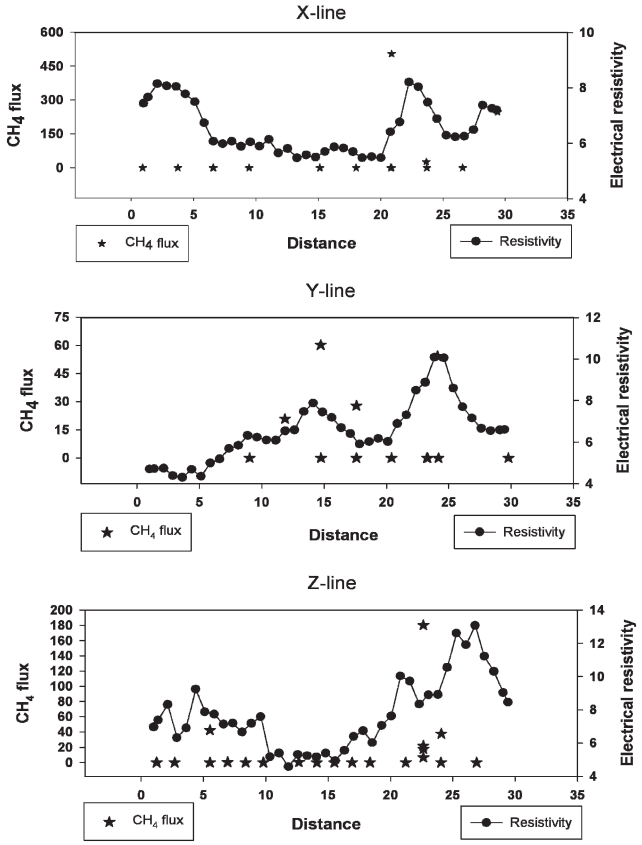

Figure 11. Spatial distribution of 2-D electrical resistivity at a depth of 1.2 m and micro-seepage of CH4 flux measured by Hong *et al.* (2009) in the WNLPA. Methane flux measurements close to X, Y, and Z lines were projected on those profiles for comparison.

measurements near the resistivity survey lines were selected and projected onto the resistivity profiles. In Fig. 11, the high resistivity regions can be correlated to the areas with high methane flux. Therefore, we concluded that the earthquake likely induced a greater-than-usual emission of gas from the gas-saturated mud fluid in fault fissures. The emitted mud fluid would have formed a thin impermeable cap and the gas would then have accumulated near the surface, resulting in the decreased water content and the higher resistivity in the vadose zone.

To estimate the change of water content in the vadose zone at the WNLPA site, we took several soil samples along the perimeter of the WNLPA site (because no sampling is allowed inside the protection zone). We conducted the "beaker test" in the laboratory to create circumstances that would enable us to identify the relationships between the water content and the resistivity at the WNLPA site. Soil samples were heated for 24 h in a 105°C oven and then packed, in equal parts, into several 1-liter beakers and weighed. The thickness of the soil samples was maintained at least 6-cm from the bottom of the beakers to ensure the absence of boundary interruptions. We added various volumes of water into the beakers and sealed the top of the beakers for a day. Next, the beakers were weighed and the resistivity was measured using a Wenner array with electrodes spaced 2-cm apart. Lastly, the soil samples were weighted again to allow correction for evaporation (loss of water) during the measurements. The beaker test provides a quick way to build the resistivity-"water content" relationships in the laboratory. In addition, the test enabled us to easily measure the oversaturated condition.

Though the WNLPA site is located in the mudstone area, the grain-size analysis shows that soil samples contained 4.0% clay, 67.1% silt, and 28.9% sand. Researchers have proposed various empirical and theoretical equations to describe the relationships between water content and measured bulk resistivity for soils and rocks, an example being Archie's empirical equation (Archie, 1942). In this study, we adopted a single power-law function similar to that of LaBrecque *et al.* (2002). The relationship between bulk resistivity and water content can then be described as

$$\rho = a \cdot \theta^{-b}, \tag{1}$$

where ρ is the bulk resistivity, θ is the volumetric water content, and a and b are the empirical constants that were determined through a comparison of measured resistivity to water content in the beaker test. Noting that parameters a and b might vary between the lab-scale test and the field experiment, we used only the empirical relationships built in the beaker test to conduct a rough evaluation of the water content's variation range at the WNLPA site. Here, we determined $a = 3.5$ and $b = 0.81$ from the unsaturated results of the beaker test shown in Fig. 12. Figure 13 shows the variations of the maximum resistivity and the estimated water content on the D and E profiles during the observation periods. After the Pingtung earthquake, the maximum resistivity increased by 10 ohm-m and 25 ohm-m on the D and E profiles (Fig. 13(a)), respectively. The estimated post-earthquake water content, however, decreased by 7% and 10% for the D and E profiles, respectively, in the vadose zone (Fig. 13(b)). The similar water-content change of the D and E profiles further indicates that the released excess gas caused by the earthquake may be the reason for the WNLPA site's change in resistivity.

Conclusions

To examine the influence of fault activities on the subsurface resistivity, we conducted a three-phase study

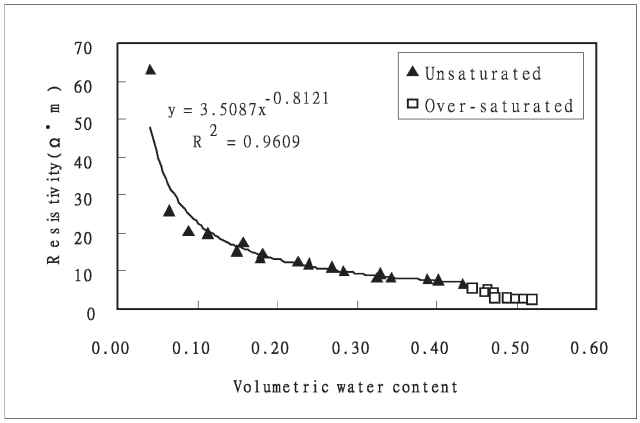

Figure 12. The relationships between the water content and the measured resistivity for the mud samples collected at the area adjacent to the WNLPA site.

at the Wushanting Natural Landscape Preservation Area site. In the first phase, we attempted to establish a geological model by conducting resistivity imaging surveys. Two isolated conductive regions were identified at a depth greater than 4-m below the surface. The positions of the conductive regions are correlated to the two mud volcano craters at the surface. The correlation suggests the locations of mud-fluid conduits in the mudstone fissures. In addition, the location of the unsaturated vadose zone is less than 4-m from the surface at the WNLPA site, and the thickness of the vadose zone decreases from the southeast corner to the northwestern part of the WNLPA.

To examine the range of short-term resistivity variation, we conducted hourly and daily measurements along a fixed survey line in the second phase of the study. The results of the hourly observations show that most of the resistivity standard deviations were less than 1 ohm-m in the 7-hour period. The hourly observations show no resistivity variation over 5 ohm-m during the study period. This finding implies that the influences from the hourly change of climate conditions were minor during the observation period. In addition to the hourly observation, the daily resistivity change varied systematically within a range of 5 ohm-m at the WNLPA site. Therefore, it appears that we can identify the long-term changes in resistivity on the basis of the short-term variations if the resistivity difference relative to the daily background is greater than 5 ohm-m.

In the third phase, we tried to evaluate whether or not the long-term resistivity variations were correlated to the local tectonic activities. During the period, the major changes of resistivity were located between the surface and a depth of 3 m. On December 26, 2006, doublet earthquakes occurred offshore near the town of Hengchun in Pingtung, about 120 km southwest from

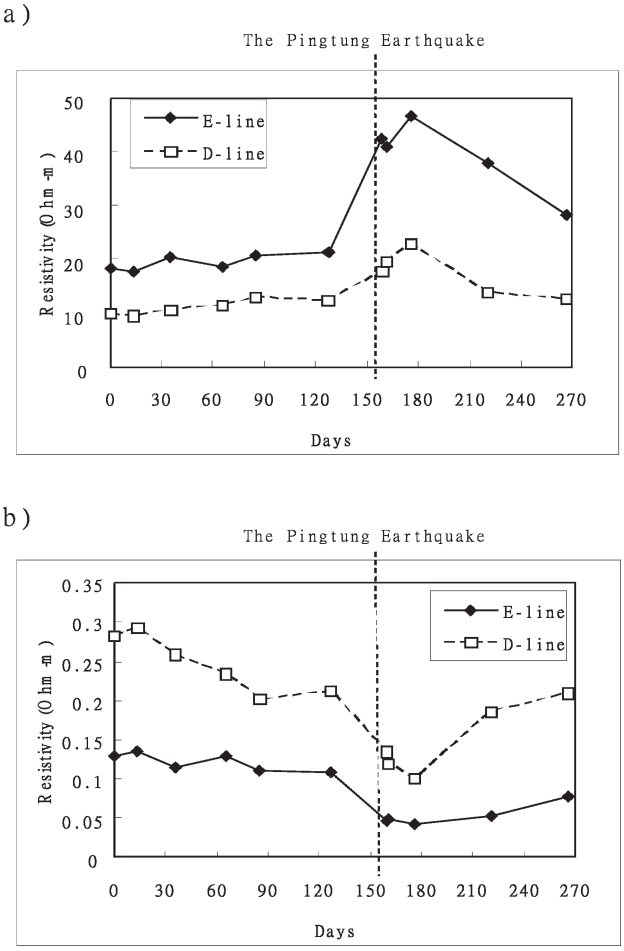

Figure 13. (a) Variation of the maximum resistivity of both the D line and the E line during the observation period. (b) Variation of the estimated water content of both the D line and the E line during the observation period.

the monitoring site. The Pingtung earthquake provided us a perfect opportunity to evaluate any change in the study area's resistivity. After the Pingtung earthquake, the maximum resistivity anomaly increased to 7 ohm-m and 20 ohm-m on two survey lines (D and E, respectively). The estimated water content decreased by 7% and 10% in the vadose zone on the D and E profiles after the earthquake. The similar water content change suggests that the released excess gas caused by the earthquake may be the reason for the decreased water content and, thus, for the increased resistivity in the vadose zone at the WNLPA site. From the results of our study, we observed that the tectonic activities may have significant influences on the vadose zone at the WNLPA site. It is reasonable to expect that the pressure wave may induce the release of a gas-saturated liquid from the saturated zone and, thus, cause the decreased water content in the vadose zone. This finding suggests that

well-controlled resistivity imaging in the vadose zone may provide researchers a useful and economical tool with which they can evaluate the potential and the actual effects of tectonic activities. Currently, we are continuing our resistivity monitoring surveys and hope to provide more data for evaluating the relationships between released gas volume and tectonic activities.

Acknowledgements

The authors would like to thank the National Science Council of the Republic of China for supporting this research under Contract No. NSC 95-2116-M-041-002 and NSC 96-2116-M-041-002.

References

AGI, 2006, Instruction Manual for EarthImager 2D ver. 2.3.0: Advanced Geosciences, Inc., Austin, Texas, 139 pp.

Archie, G.E., 1942, The electrical resistivity log as an aid in determining some reservoir characteristics: American Institute of Mining and Metallurgy, **146**, 54–62.

Chen, H.Y., Lee, J.C., Kuo, L.C., Yu, S.B., and Liu, C.C., 2008, Coseismic surface GPS displacement and ground shaking associated with the 2006 Pingtung earthquake doublet, offshore southern Taiwan: Terr. Atmos. Ocean. Sci., **19**(6) 683–696.

Chow, J.J., Chang, S.K., and Yu, H.S., 2006, GPR reflection characteristics and depositional models of mud volcanic sediments—Wushanting mud volcano field, southwestern Taiwan: Journal of Applied Geophysics, **60**, 179–200.

CWB, 2006, Earthquake Report 107: The Central Weather Bureau, Taipei, Taiwan. http://www.cwb.gov.tw/V5e/index.htm.

Fertl, W.H., and Tinmo, D.J., 1970, Occurrence and significance of abnormal-pressure formations: Oil and Gas Journal, **5**, 97–108.

Garambois, S., Sénéchal, P., and Perroud, H., 2002, On the use of combined geophysical methods to assess water content and water conductivity of near-surface formations: Journal of Hydrology, **259**, 32–48.

Hedberg, H.D., 1980, Methane generation and petroleum migration *in* Problems of petroleum migration: Geologist studies in geology 10, Roberts, W.H., and Cordell, R.J. (eds.), The American Association of Petroleum Geologist, Tulsa, 179–206.

Higgins, G.E., and Saunders, J.B., 1974, Mud volcanoes: their nature and origin: Contribution to geology and paleobiology of the caribbean and adjacent areas: Verhandlungen Naturforschenden Gesellschaft Basel, **84**, 101–152.

Hong, W.L., Etiope, G., Yang, T.F., and Chang, P.Y., 2009. Methane micro-seepage in European and Asian mud volcanoes, submitted to the Journal of Asian Earth Sciences.

Huang, I.L., Teng, L.S., Liu, C.S., Reed, D.L., and Lundberg, N., 1992, Structural styles of offshore southwestern Taiwan: EOS, **73**, 539.

Kean, W.F., Walter, M.J., and Layson, H.R., 1987, Monitoring moisture migration in the vadose zone with resistivity: Groundwater, **25**, 562–571.

Keng, W.P., 1981, Geologic map of Tainan Hills: Bulletin of the Central Geological Survey, **1**, 1–31.

LaBrecque, D., Alumbaugh, D.L., Yang, Y., Paprocki, L., and Brainard, J., 2002, Three-dimensional monitoring of vadose zone infiltration using electrical resistivity tomography and cross-borehole ground penetrating radar *in* Three-dimensional electromagnetic Methods: Geochemistry and Geophysics 35, Zhdanov, M.S., and Wannermaker, P.E. (eds.), Elsevier Applied Science Publishers, Ltd., London, 260–272.

Liu, C.S., Huang, I.L., and Teng, L.S., 1997, Structural features off southwestern Taiwan: Marine Geology, **137**, 305–319.

Lippmann, E., 2005. Four-point light hp technical data and operating instructions ver. 3.37: Lipmann Geophysikalische Messgeräte, Schaufling, Germany, 29 pp.

Reed, D.L., Silver, E.R., Tagudin, J.E., Shipley, T.H., and Vrolijk, P., 1990, Relations between mud volcanoes, thrust deformation, slope sedimentation, and gas hydrate, offshore north Panama: Marine and Petroleum Geology, **7**, 44–54.

Shih, T.T., 1967, A survey of the active mud volcanoes in Taiwan and a study of their types and the character of the mud: Petroleum Geology Taiwan, **5**, 259–311.

Sung, Q.C., Chen, L., and Chen, Y.C., 2004, Some new observations about the Chishan Fault: Di-Chi, **23**, 31–40 (in Chinese).

Telford, W.M., Geldart, L.P., Sheriff, R.E., and Keys, D.A., 1990, Applied Geophysics, 2nd ed.: Cambridge University Press, London, 860 pp.

Van, G.P., Park, S.K., and Hamilton, O., 1991, Monitoring leaks from storage ponds using resistivity methods: Geophysics, **56**, 1267–1270.

Wang, S., Shu, M., and Yang, C., 1988, Morphological study of mud volcanoes on land in Taiwan: Journal of Natural Taiwan Museum, **31**, 31–49.

Yang, C.H., Cheng, P.H., You, J.I., and Tsai, L.L., 2002, Significant resistivity changes in the fault zone associated with the 1999 Chi-Chi earthquake, west-central Taiwan: Tectonophysics, **350**, 299–313.

You, C.F., Gieskes, J., Lee, M.T., Yui, T.F., and Chen, H.W., 2004, Geochemistry of mud volcano fluids in the Taiwan accretionary prism: Applied Geochemistry, **19**, 695–707.